

Testing the Applicability of the Official Croatian DTM for Normalization of UAV-based DSMs and Plot-level Tree Height Estimations in Lowland Forests

Ivan Balenović, Luka Jurjević, Anita Simić Milas, Mateo Gašparović, Danijela Ivanković, Ante Seletković

Abstract

The Airborne Laser Scanning (ALS) technology has been implemented in operational forest inventories in a number of countries. At the same time, as a cost-effective alternative to ALS, Digital Aerial Photogrammetry (PHM), based on aerial images, has been widely used for the past 10 years. Recently, PHM based on Unmanned Aerial Vehicle (UAV) has attracted great attention as well. Compared to ALS, PHM is unable to penetrate the forest canopy and, ultimately, to derive an accurate Digital Terrain Model (DTM), which is necessary to normalize point clouds or Digital Surface Models (DSMs). Many countries worldwide, including Croatia, still rely on PHM, as they do not have complete DTM coverage by ALS (DTM_{ALS}). The aim of this study is to investigate if the official Croatian DTM generated from PHM (DTM_{PHM}) can be used for data normalization of UAV-based Digital Surface Model (DSM_{UAV}) and estimating plot-level mean tree height (H_L) in lowland pedunculate oak forests. For that purpose, H_L estimated from DSM_{UAV} normalized with DTM_{PHM} and with DTM_{ALS} were generated and compared as well as validated against field measurements. Additionally, elevation errors in DTM_{PHM} were detected and eliminated, and the improvement by using corrected DTM_{PHM} (DTM_{PHMc}) was evaluated. Small, almost negligible variations in the results of the leave-one-out cross-validation were observed between H_L estimated using proposed methods. Compared to field data, the relative root mean square error (RMSE_{rel}) values of H_L estimated from DSM_{UAV} normalized with DTM_{ALS} , DTM_{PHM} and DTM_{PHMc} were 5.10%, 5.14%, and 5.16%, respectively. The results revealed that in the absence of DTM_{ALS} , the existing official Croatian DTM could be readily used in remote sensing based forest inventory of lowland forest areas. It can be noted that DTM_{PHMc} did not improve the accuracy of H_L estimates because the gross errors mainly occurred outside of the study plots. However, since the existence of the gross errors in Croatian DTM_{PHM} has been confirmed by several studies, it is recommended to detect and eliminate them prior to using the DTM_{PHM} in forest inventory.

Keywords: Unmanned Aerial Vehicle, Digital Aerial Photogrammetry, Airborne Laser Scanning, Digital Surface Model, Digital Terrain Model, forest inventory

1. Introduction

Data collected during forest inventory are critical for sustainable forest management. In addition to classical, labour-intensive and time-consuming field measurements, information about forests can be collected

using various remote sensing methods (White et al. 2016). The most efficient RS technology in terms of accuracy is Airborne Laser Scanning (ALS) based on Light Detection and Ranging (LiDAR), as confirmed by a number of studies over the past 20 years (Næsset 1997, 2002, Coops et al. 2007, Yu et al. 2010, Rahlf et al.

2014, Montealegre et al. 2016, Ullah et al. 2017, Smreček et al. 2018, Ørka et al. 2018). As a result, the ALS technology has been implemented in operational forest inventories of a number of countries (Næsset 2014, Ørka et al. 2018). From ALS point clouds, the height and density metrics describing forest structure are calculated. By applying the commonly used Area Based Approach (ABA), in which ALS metrics of a certain number of sample plots are regressed against field reference data to establish prediction models, different forest inventory variables for a targeted forest area could be obtained. However, the high-acquisition costs of ALS are a limiting factor for using this technology in forest inventory of many countries.

As a cost-effective alternative to ALS technology, Digital Aerial Photogrammetry (PHM), based on aerial images obtained by aircraft (White et al. 2013), has attracted great attention in forest inventory research over the past 10 years (Baltsavias et al. 2008, Bohlin et al. 2012, 2017, Straub et al. 2013, Stepper et al. 2015, Balenović et al. 2017, Rahlf et al. 2017, Ullah et al. 2017, Zimmermann and Hoffmann 2017). More recently, PHM using an Unmanned Aerial Vehicle (UAV) has also attracted great attention in forest inventory studies (Lisein et al. 2013, Puliti et al. 2015, 2017, Tuominen et al. 2015, 2017, Wallace et al. 2016, Gašparović et al. 2017, Goodbody et al. 2017, Guerra-Hernández et al. 2017, 2018, Ota et al. 2017).

Compared to ALS, PHM is unable to penetrate through the forest canopy and to derive an accurate Digital Terrain Model (DTM) (White et al. 2013), especially during the leaf-on conditions. The accuracy of DTMs, such as those derived by ALS, is necessary to normalize point clouds or Digital Surface Models (DSMs) derived by PHM, when converting elevations to height-above-ground values. In most of the above-mentioned UAV studies (Lisein et al. 2013, Puliti et al. 2015, 2017, Tuominen et al. 2015, 2017, Ota et al. 2017, Goodbody et al. 2017, Ota et al. 2017), which aimed to predict tree and forest variables, point clouds or DSMs were normalized with ALS-derived DTM (DTM_{ALS}). In several other studies (Wallace et al. 2016, Guerra-Hernández et al. 2017, 2018) authors created and used DTM from UAV point clouds and confirmed the well-known fact that those DTMs can be of high accuracy only in areas of relatively low canopy closure with a greater proportion of visible ground. Therefore, the accuracy of photogrammetric DTM can be increased by using images collected during the leaf-off conditions (DeWitt et al. 2017, Moudry et al. 2018).

Many countries still do not have complete DTM_{ALS} coverage. For example, in Croatia, only several ALS surveys over small areas have been conducted in re-

cent years. The existing digital terrain data were primarily collected by using manual stereo-photogrammetric methods and aerial images, supported with vectorization of existing maps and field data collection, and they represent the national standard and the only available DTM data for the entire Croatian territory. Since the accuracy of such 'photogrammetric' DTM (DTM_{PHM}) in forest areas is questionable, Balenović et al. (2018) evaluated its vertical accuracy in lowland pedunculate oak (*Quercus robur* L.) forests and concluded that in the absence of DTM_{ALS} , DTM_{PHM} could be used in lowland forest areas, but with the greatest caution. Namely, Balenović et al. (2018) revealed the presence of gross errors in terrain data, which considerably affected the DTM_{PHM} accuracy, and had to be eliminated from terrain data prior to the DTM_{PHM} generation.

The aim of the present study is to investigate if such DTM_{PHM} can be used in combination with UAV DSM (DSM_{UAV}) for plot-level remote sensing based forest inventory in lowland pedunculate oak forests. For that purpose, plot-level mean tree heights estimated from DSM_{UAV} normalized with DTM_{PHM} as well as with DTM_{ALS} were compared to field estimated mean tree heights. Additionally, elevation errors in DTM_{PHM} were eliminated using the method proposed by Gašparović et al. (2018) and estimates from DSM_{UAV} normalized with the corrected DTM_{PHM} ($DTM_{PHM(c)}$) was also evaluated.

2. Materials and methods

2.1 Study area

The study area covers a 411.30 ha of even-aged pedunculate oak forests of »Jastrebarski lugovi« management unit located in Central Croatia, approximately 35 km southwest of Zagreb (Fig. 1). The area is a part of a larger Pokupsko Basin lowland forest complex (≈12 000 ha). The even-aged oak stands of the study area are mixed with other tree species such as common hornbeam (*Carpinus betulus* L.), black alder (*Alnus glutinosa* (L.) Geartn.), and narrow-leaved ash (*Fraxinus angustifolia* Vahl.). Two understory species, common hazel (*Corylus avellana* L.) and common hawthorn (*Crataegus monogyna* Jacq.), are present in the entire area. These forests are state-owned and they are actively managed for sustained timber. The terrain is flat with ground elevations ranging from 105 to 118 m a.s.l.

2.2 Field data

Field data were collected in 2017. A total of 105 circular sample plots with a radius of 8 or 15 m

depending on the stand age were set in 19 oak stands (subcompartments). Out of 105 sample plots, 44 were located in oak stands of age class 3 (41–60-year-old), 36 in stands of age class 4 (61–80-year-old), 13 in stands of age class 5 (81–100-year-old), and 12 plots in stands of age class 7 (>121-year-old). The selected sample

plots belong to a larger set of permanent, systematically distributed plots, which cover a somewhat larger area. The available ALS data do not cover the entire area of Pokupsko Basin and, therefore, only plots for which both DTM_{ALS} and DTM_{PHM} existed were selected for this study. The methodology of setting up the

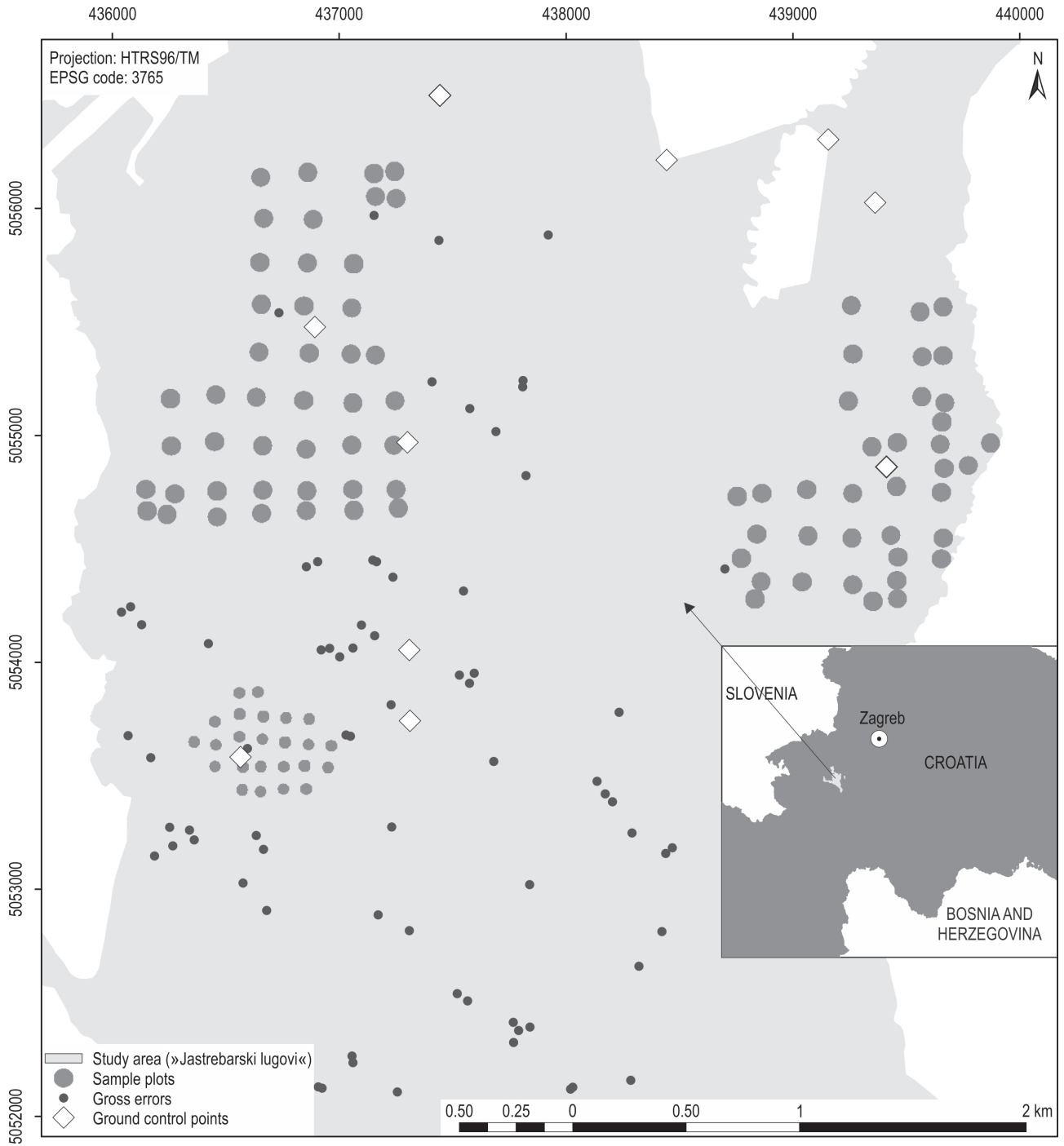


Fig. 1 Location of the study area («Jastrebarski lugovi» management unit) in Croatia with: spatial distribution of field sample plots, gross (elevation) errors detected and eliminated from DTM_{PHM} and ground control points used for UAV images orientation

systematic grid (100×100 m, 100×200 m, 200×100 m, or 200×200 m) of sample plots throughout the study area was described in Balenović et al. (2018).

The coordinates of the plot centres were recorded using the Global Navigation Satellite System (GNSS) receiver Stonex S9IIN connected with the Croatian Positioning System (CROPOS), i.e., the Real-Time Kinematic (RTK) positioning technique was applied. The average precision of the positioning was 0.13 m (i.e. standard deviation calculated by the receiver). Within each plot, tree species were recorded and diameters at breast height (DBH) were measured for all trees with DBH≥10 cm. Tree height was measured for at least 50% trees per plot using the Vertex III hypsometer. An attempt was made to achieve an equal distribution of sampled trees including the whole range of species and DBH values present at each plot. Out of 3384 sampled trees, tree height was measured for 2263 trees (66.87%). To estimate tree height of remaining trees, the species-specific BDH-height models fitted with Michailoff's function (Michailoff 1943) were developed. Lorey's mean height (H_L) of each plot was calculated as:

$$H_L = \frac{\sum h_i \times g_i}{G_{\text{plot}}} \quad (1)$$

Where:

- h_i tree height of a single (i) tree at the plot, m
- g_i basal area of an i tree at the plot, m²
- G_{plot} plot basal area, m².

The main characteristics of the surveyed plots are presented in Table 1.

2.3 Digital terrain models (DTMs)

2.3.1 Airborne Laser Scanning DTM (DTM_{ALS})

The DTM_{ALS} was provided by the Hrvatske Vode Ltd. (Zagreb, Croatia) in the raster format with a spatial resolution of 0.5 m. The acquisition and processing

of the airborne LiDAR data were done by the Institute for Photogrammetry Inc. (Zagreb, Croatia) and Mensuras Ltd. (Maribor, Slovenia). The ALS data were collected with an Optech ALTM Gemini 167 laser scanner mounted on the Pilatus P6 aircraft under the leaf-on conditions in several surveys between 29 June and 25 August 2016. The resulting point densities considering »all returns« and the »last return« were 13.64 points·m⁻² and 9.71 points·m⁻², respectively. The ALS point data were classified using TerraSolid software version 11 (Terrasolid Ltd. 2012), into ASPRS Standard LiDAR Point Classes (ASPRS 2008). Approximately 7% of all returns over the study area were classified as »ground« based on the progressive Triangulated Irregular Network (TIN) densification algorithm (Axelsson 2000), resulting in average ground point density of 0.91 points·m². A raster DTM_{ALS} with a spatial resolution of 0.5 m was generated from the classified ground returns. The vertical accuracy of the same DTM_{ALS} was evaluated in the recent study of Balenović et al. (2018). The obtained root mean square error (RMSE), mean error (ME), and standard deviation (SD) for DTM_{ALS} were 0.14 m, 0.09 m, and 0.10 m, respectively. More details on LiDAR sensor, data processing and DTM_{ALS} characteristics can be found in Balenović et al. (2018).

2.3.2 Photogrammetric DTM (DTM_{PHM})

DTM_{PHM} in the raster format with a spatial resolution of 0.5 m was generated from the official digital terrain data for the territory of Croatia with the TIN and linear interpolation techniques using the Global Mapper software (ver. 19, Blue Marble Geographics, Hallowell, Maine, USA). These vector data (breaklines, formlines, spot heights, and mass points) represent the Croatian national standard and, currently, they are the only available DTM data for the entire Croatian territory. The data were primarily obtained from aerial images with the GSD of ≤30 cm using manual stereo photogrammetric

Table 1 Summary of the plot-level field data (mean and standard deviation values) for the main structural parameters

Age Class	<i>N</i> of plots	DBH, cm	H_L , m	<i>N</i> , trees·ha ⁻¹	<i>G</i> , m ² ·ha ⁻¹	<i>V</i> , m ³ ·ha ⁻¹
3	44	22.7 ± 3.8	22.8 ± 2.4	808 ± 369	29.7 ± 6.8	329.5 ± 77.0
4	36	28.4 ± 4.2	25.3 ± 2.2	497 ± 118	30.5 ± 5.3	395.3 ± 103.5
5	13	32.6 ± 4.6	26.0 ± 3.0	442 ± 150	35.0 ± 6.5	467.6 ± 127.8
7	12	30.0 ± 5.3	27.2 ± 3.3	561 ± 153	39.5 ± 14.0	527.4 ± 244.9

DBH – mean diameter by basal area
 H_L – Lorey's mean height
N – number of trees
G – basal area
V – volume grouped in age classes

methods, and supported with vectorization of existing maps and field data collection. A detailed description of digital terrain data can be found in Balenović et al. (2018). According to results of the accuracy assessment conducted in the study of Balenović et al. 2018, the RMSE, ME, and SD for DTM_{PHM} of 5 m resolution were 0.35 m, 0.17 m, and 0.31 m, respectively.

2.3.3 Corrected (improved) photogrammetric DTM (DTM_{PHMc})

Within the above-mentioned study (Balenović et al. 2018), authors discovered the presence of a certain number of outliers (i.e., gross errors) in the official Croatian digital terrain data, which considerably affected the accuracy of generated DTM_{PHM} . Therefore, elevation errors in DTM_{PHM} were eliminated using the automatic method proposed by Gašparović et al. (2018). By combining slope and tangential curvature values of raster DTM_{PHM} , the method automatically detected and eliminated 91 outliers or 3.2% of the total number of source points within the study area, and such corrected DTM_{PHMc} was also used in this study.

2.4 UAV data

The UAV images were acquired using the fixed-wing Trimble UX5 HP with Sony Alpha 7R camera on 30 and 31 May 2017. The study area was covered by 1441 images with the ground sampling distance (GSD) of ≈ 8 cm. The images were collected in 4 flights with endlap of 90% and sidelap of 80%.

Prior to the UAV survey, 10 ground control points (GCPs) were placed and measured across the study area (Fig. 1). The GCPs' positions were measured us-

ing the Trimble GNSS receiver connected with the CROPOS (RTK positioning). Due to dense forest, GCPs were set up and measured along the forest roads from where they were easily detected on UAV images, which consequently led to somewhat irregular distribution of the points. Therefore, to provide accurate image position, dual-frequency GNSS data collected by the UAV were post-processed with the Post-Processed Kinematic (PPK) method using the Virtual Reference Station (VRS) data obtained from the Croatian State Geodetic Administration.

2.5 Photogrammetric processing (DSM generation)

The block of UAV images was processed using the PHOTOMOD UAS 6.3 digital photogrammetric system (Racurs Co., Moscow, Russia). A raster DSM of 10 cm spatial resolution from UAV images was generated using the Dense DSM algorithm (Semi-Global Matching method) of PHOTOMOD software. Besides the default parameters settings, the »Median filter« was applied with threshold and aperture values of 0.01 m and 3, respectively. In order to allow further processing (plot-level metrics extraction), a raster DSM was converted into a point format. By applying the »thin-out« coefficient of 1, the spatial resolution, i.e. grid size of points (10×10 cm) remained identical to the pixel size of the initial raster DSM.

2.6 Variables (plot-level metrics) extraction

The plot-level metrics, which are commonly used as independent variables in forest attributes modelling,

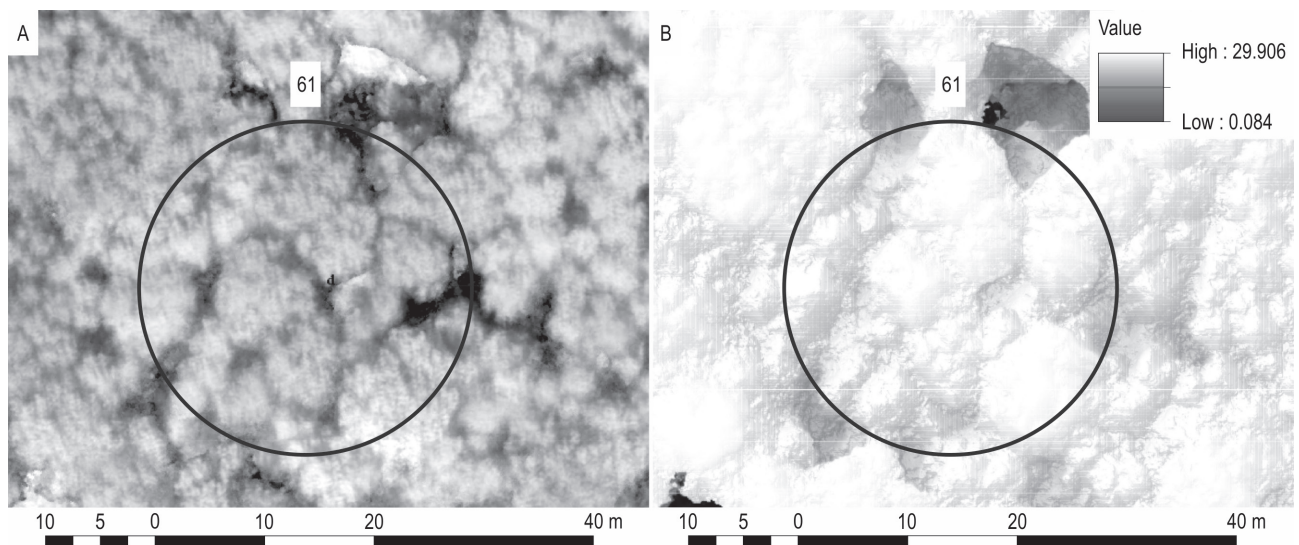


Fig. 2 Digital orthophoto (A), and DSM normalized with $DTM_{ALS} - nDSM_{U-A}$ (B) for one exemplary plot

were obtained using the FUSION LDV 3.70 open source software (McGaughey 2014). First, DSM_{UAV} in point format was normalized with three different DTMs (DTM_{ALS} , DTM_{PHM} , and DTM_{PHMc}) in order to obtain aboveground heights. In this way, three different normalized DSMs (nDSMs) were obtained: $nDSM_{U-A}$ (DSM_{UAV} normalized with DTM_{ALS}) (Fig. 2), $nDSM_{U-P}$ (DSM_{UAV} normalized with DTM_{PHM}), and $nDSM_{U-Pc}$ (DSM_{UAV} normalized with DTM_{PHMc}). The nDSMs were then clipped to the spatial extent of each field plot, and a set of statistical plot-level metrics was generated. During the metrics extraction, the minimum height threshold of 2 m was applied to remove ground and understorey vegetation (e.g., shrubs, small trees with $DBH < 10$ cm). In order to calculate additional canopy cover metrics, the height break thresholds of 5 m, 10 m, 15 m, 20 m, and 25 m were also applied. In total, 39 metrics arranged in four groups (height metrics, height percentiles, height variability, and canopy cover metrics) were extracted and considered in the statistical modelling as potential independent variables (Table 2).

2.7 Development and validation of plot-level mean tree height (H_L) models

In order to reduce a large number of potential independent variables considered for development of plot-level models for mean tree height estimation, a two-step pre-selection approach was applied. In the first step, the number of potential independent variables was reduced based on Pearson correlation coefficient (r). Only variables that were highly correlated with field H_L ($r \geq \pm 0.5$) were included in the collinearity analysis. Separately for each group of variables, r was calculated between the remaining variables and threshold of $r \geq \pm 0.7$ (Dormann et al. 2013) was applied to further eliminate some variables from the analysis (multivariate linear regression). By applying the backward stepwise regression, the best-fit model was developed and selected for each nDSM ($nDSM_{U-A}$, $nDSM_{U-P}$, $nDSM_{U-Pc}$) using the whole dataset (105 sample plots). Plot-level height models were validated using the leave-one-out cross-validation (LOOCV) approach (Montealegre et al. 2016, Puliti et al. 2016) and field H_L . The adjusted coefficient of determination (R^2_{adj}) and graphical analyses (observed vs. predicted values) were used to evaluate the goodness-of-fit of the plot-level H_L models, whereas the accuracy of the model estimates were evaluated using the root mean square error ($RMSE$), relative root mean square error ($RMSE_{\%}$), mean error (ME), and relative mean error ($ME_{\%}$):

$$RMSE = \sqrt{\frac{\sum_{i=1}^n (H_{L'i} - H_L)^2}{n}} \quad (2)$$

$$RMSE_{\%} = \frac{RMSE}{H_L} \times 100 \quad (3)$$

$$ME = \frac{\sum_{i=1}^n (H_{L'i} - H_L)}{n} \quad (4)$$

$$ME_{\%} = \frac{ME}{H_L} \times 100 \quad (5)$$

Where:

$H_{L'i}$ predicted (UAV estimated) Lorey's mean height of plot i

H_L observed (from field data) Lorey's mean height of plot i

n number of plots

$\frac{1}{H_L}$ mean of the observed values.

A two-step pre-selection of independent variables and backward stepwise regression were carried out using STATISTICA 11 (Hill and Levicki 2007), whereas LOOCV was performed in MATLAB (MathWorks 2016).

3. Results and discussion

Pearson correlation coefficients (r) between the plot-level H_L estimated from field measurements and metrics extracted from three different nDSMs are presented in Table 2. All observed metrics yielded very similar r values for all nDSMs. The strongest correlation with H_L was obtained for h_{max} (0.84 for all nDSMs), $CURT_mean_CUBE$ (0.69–0.71), P_{99} (0.89 for all nDSMs), and $Per_{>25}$ (0.79 for all nDSMs), for height metrics, height variability metrics, height percentiles, and canopy cover metrics, respectively.

After applying a two-step pre-selection approach, six similar almost identical metrics (variables) were selected and included in the backward stepwise regression for all nDSMs. While for the $nDSM_{U-A}$ h_{max} , h_{mean} , $CURT_mean_CUBE$, P_{70} , P_{99} , and $Per_{>25}$ were selected and included, for both $nDSM_{U-P}$ and $nDSM_{U-Pc}$ h_{max} , h_{mean} , $CURT_mean_CUBE$, P_{75} , P_{99} , and $Per_{>25}$ were selected and included in regression analyses. Accordingly, the only difference is that P_{70} was selected for $nDSM_{U-A}$ modelling, whereas P_{75} was selected for both $nDSM_{U-P}$ and $nDSM_{U-Pc}$ modelling.

For each nDSM, the best-fit plot-level H_L linear model was developed and selected based on the backward stepwise regression (Table 2) of previously

Table 2 Results of a two-step approach for pre-selection of potential independent variables considered for development of plot-level H_L models. Pearson correlation coefficients (r) between the plot-level metrics extracted from DSM_{UAVs} (and normalized with three different DTMs) and plot-level H_L from field measurements

Variable	Description	H_L		
		nDSM _{U-A}	nDSM _{U-P}	nDSM _{U-Pc}
Height metrics				
h_min	Minimum height	-0.0028 ^{ns}	-0.0191 ^{ns}	-0.0194 ^{ns}
h_max	Maximum height	0.8395 ^{***}	0.8357 ^{***}	0.8364 ^{***}
h_mean	Mean height	0.5983 ^{***}	0.5710 ^{***}	0.5709 ^{***}
h_mode	Mode height	0.5017 ^{**}	0.4931 ^{**}	0.5023 ^{**}
Height variability metrics				
SD	Standard deviation	0.3850 [*]	0.3857 [*]	0.3868 [*]
VAR	Variance	0.3541 [*]	0.3543 [*]	0.3554 [*]
CV	Coefficient of variation	0.14318	0.1416 ^{ns}	0.1425 ^{ns}
IQ	Interquartile distance	0.3607 [*]	0.3604 [*]	0.3606 [*]
Skew	Skewness	-0.2153 [*]	-0.2142 [*]	-0.2125 [*]
Kurt	Kurtosis	0.0094 ^{ns}	0.0105 ^{ns}	0.0106 ^{ns}
AAD	Average Absolute Deviation	0.3865 [*]	0.3869 [*]	0.3879 [*]
MAD-med	Median of absolute deviations from overall median	0.3076 [*]	0.3089 [*]	0.3090 [*]
MAD-mode	Median of absolute deviations from overall mode	0.1758 ^{ns}	0.1800 ^{ns}	0.1832 ^{ns}
CRR	Canopy relief ratio ((mean – min) / (max – min))	0.2316 [*]	0.2311 [*]	0.2263 [*]
SQRT_mean_SQ	Generalized mean for the 2nd power (Elevation quadratic mean)	0.6575 ^{**}	0.6321 ^{**}	0.6322 ^{**}
CURT_mean_CUBE	Generalized mean for the 3rd power (Elevation cubic mean)	0.7083 ^{***}	0.6852 ^{***}	0.6856 ^{***}
Height percentiles				
P ₀₁	1st percentile	0.0405 ^{ns}	0.0221 ^{ns}	0.0208 ^{ns}
P ₀₅	5th percentile	0.1323 ^{ns}	0.1144 ^{ns}	0.1132 ^{ns}
P ₁₀	10th percentile	0.2072 [*]	0.1877 [*]	0.1866 [*]
P ₂₀	20th percentile	0.3154 [*]	0.2956 [*]	0.2949 [*]
P ₂₅	25th percentile	0.3657 [*]	0.3469 [*]	0.3467 [*]
P ₃₀	30th percentile	0.4014 [*]	0.3828 [*]	0.3827 [*]
P ₄₀	40th percentile	0.5028 ^{**}	0.4861 [*]	0.4862 [*]
P ₅₀	50th percentile	0.5670 ^{**}	0.5519 ^{**}	0.5518 ^{**}
P ₆₀	60th percentile	0.6256 ^{**}	0.6107 ^{**}	0.6109 ^{**}
P ₇₀	70th percentile	0.6885 ^{***}	0.6763 [*]	0.6765 ^{**}
P ₇₅	75th percentile	0.7208 ^{**}	0.7101 ^{***}	0.7104 ^{***}
P ₈₀	80th percentile	0.7583 ^{**}	0.7515 ^{**}	0.7518 ^{**}
P ₉₀	90th percentile	0.8170 ^{**}	0.8134 ^{**}	0.8138 ^{**}
P ₉₅	95th percentile	0.8627 ^{**}	0.8610 ^{**}	0.8615 ^{**}
P ₉₉	99th percentile	0.8877 ^{***}	0.8886 ^{***}	0.8893 ^{***}
Canopy cover metrics				
Per _{>2}	Percentage of pixels/points above 2 m	0.0822 ^{ns}	0.0884 ^{ns}	0.0885 ^{ns}
Per _{>mean}	Percentage of pixels/points above the mean height	0.2372 [*]	0.2402 [*]	0.2356 [*]
Per _{>mode}	Percentage of pixels/points above the mode height	-0.0951 ^{ns}	-0.0903 ^{ns}	-0.1291 ^{ns}
Per _{>5}	Percentage of pixels/points above 5 m	0.1117 ^{ns}	0.1180 ^{ns}	0.1182 ^{ns}
Per _{>10}	Percentage of pixels/points above 10 m	0.0734 ^{ns}	0.0780 ^{ns}	0.0783 ^{ns}
Per _{>15}	Percentage of pixels/points above 15 m	0.0446 ^{ns}	0.0467 ^{ns}	0.0428 ^{ns}
Per _{>20}	Percentage of pixels/points above 20 m	0.4638 [*]	0.4317 [*]	0.4264 [*]
Per _{>25}	Percentage of pixels/points above 25 m	0.7919 ^{***}	0.7922 ^{***}	0.7919 ^{***}

ns – correlation is not statistically significant ($p < 0.05$) → variable is excluded from further analyses

* correlation is statistically significant ($p < 0.05$) but $r < \pm 0.5$ → variable is excluded from further analyses

** correlation is statistically significant ($p < 0.05$) with $r > \pm 0.5$ → variable is included in collinearity analyses

*** variables selected for inclusion in a multivariate linear regression (backward stepwise) based on a collinearity analyses conducted for each group of variables separately

Table 3 Plot-level H_L models developed using multivariate linear regression (backward stepwise) and results of leave-one-out cross-validation

nDSM	Model	R^2_{adj}	RMSE, m	RMSE _% , %	ME, m	ME _% , %
nDSM _{U-A}	$H_L = 5.4105 + 0.6728 \cdot P_{99} + 0.0351 \cdot Per_{>25}$	0.8160	1.2509	5.0966	-0.0009	-0.0040
nDSM _{U-P}	$H_L = 4.8094 + 0.6919 \cdot P_{99} + 0.0358 \cdot Per_{>25}$	0.8129	1.2617	5.1404	0.0602	0.2454
nDSM _{U-Pc}	$H_L = 4.7235 + 0.6963 \cdot P_{99} + 0.0349 \cdot Per_{>25}$	0.8116	1.2659	5.1578	0.1156	0.4710

selected potential independent variables (Table 3) and field H_L in the 105 sample plots. Identical independent variables were included in all three models. Each model included one height percentile (P_{99}) and one canopy cover metric ($Per_{>25}$). All models, as well as their parameters, were highly significant ($p < 0.001$). Small, almost negligible variations in the results of LOOCV were observed between all three models (Table 3). However, according to LOOCV, the model for nDSM_{U-A} had the best performance producing the highest prediction accuracy (R^2_{adj}) and the least errors (RMSE, RMSE_%, ME, ME_%). It was followed by the model for nDSM_{U-P}, which showed slightly worse performance, while the model for nDSM_{U-Pc} had the worst performance. Furthermore, according to ME and ME_% values, model for nDSM_{U-A} on average slightly underestimated, whereas models for both nDSM_{U-P} and nDSM_{U-Pc} slightly overestimated field estimated H_L . Very similar performance of all three models was also confirmed in the scatterplots (Fig. 3).

The results of this study confirmed the findings of previous studies, which emphasized the great potential of UAV photogrammetry in ABA forest inventory.

For example, Puliti et al. (2015) used point clouds metrics and spectral characteristics of images to estimate various plot-level variables in conifer dominated boreal forests in Norway. For H_L estimation, they used linear model with P_{20} , SD and mean of the green band. LOOCV conducted on 38 sample plots revealed R^2_{adj} of 0.71 and RMSE_% of 13.3%. Ota et al. (2017) performed research in temperate coniferous plantations in Japan. According to LOOCV for 20 rectangular plots, the linear model with P_{90} and dominant tree type as independent variables showed the best accuracy ($R^2_{adj}=0.93$, RMSE_{%}=6.65%), while the attempt to include the spectral characteristics did not result in accuracy improvements. Furthermore, Tuominen et al. (2017) used point cloud metrics and both spectral and textural features extracted from hyperspectral UAV images to estimate attributes of 298 sample plots in conifer dominated boreal forests in Finland. By using K-nearest neighbour estimation method and generic algorithm for selecting an appropriate set of features, they estimated H_L with RMSE_% of 7.4%.}

Although in the present study H_L modelling was based solely on nDSMs metrics (Table 2), slightly to

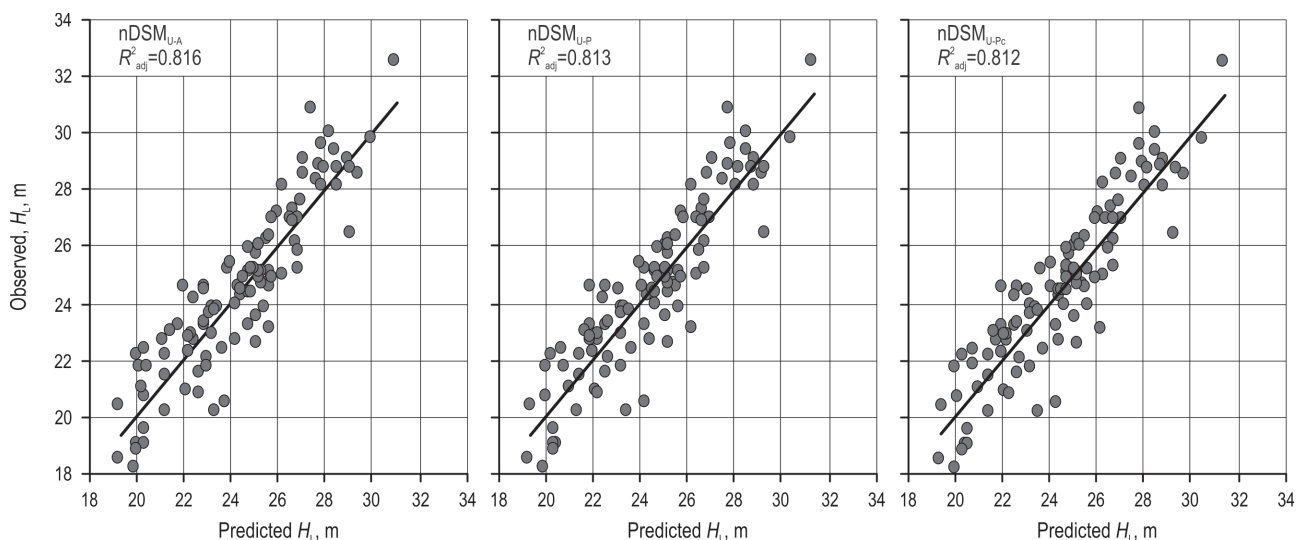


Fig. 3 Observed vs. predicted Lorey's mean height (H_L) for three selected plot-level (leave-one-out cross-validation) described in Table 3. The solid line represents fitted linear model

considerably better accuracy of H_L estimates was achieved (Table 3) compared to previous studies, which, in addition to point cloud metrics, used spectral (Puliti et al. 2015, Tuominen et al. 2017) and textural (Tuominen et al. 2015, 2017) features of orthoimages or additional data such as dominant tree type (Ota et al. 2017). It is important to emphasize that all above-mentioned studies used DTM_{ALS} for normalization of UAV point clouds, whereas two of tree DSMs in this study were normalized with the official Croatian DTM_{PHM} . However, direct comparison between the studies is difficult due to a number of differences, such as forest structure and site characteristics, UAV and camera characteristics, flight conditions, and photogrammetric software. To the best of authors' knowledge, this is the first study that investigates the capability of UAV photogrammetry in forest inventory of lowland even-aged pedunculate oak forests.

Furthermore, the obtained results are also in agreement with the previous studies based on ALS data or digital aerial images obtained by aircraft. According to several comparison studies (Nurminen et al. 2013, Vastaranta et al. 2013, Pitt et al. 2014, Gobakken et al. 2015), the $RMSE_{\%}$ values for H_L estimated using ALS data and digital aerial images ranged from 6.5% to 7.8%, and from 6.6% to 11.2%, respectively. However, for direct comparison of the UAV technology with ALS or PHM based on digital aerial images, it would be necessary to conduct the research on the same area of interest.

This study confirms the findings of previous studies (Balenović et al. 2017, 2018) that in the absence of DTM_{ALS} , the existing official Croatian DTM_{PHM} could be readily used in remote sensing based forest inventory of lowland forest areas. Furthermore, it can be noted that DTM_{PHMc} did not improve the accuracy of H_L estimates, primarily because the eliminated gross errors did not occur within the plots used in the analysis (Fig. 3). However, the existence of gross errors in the official Croatian digital terrain data DTM_{PHM} has been confirmed by several studies (Balenović et al. 2018, Gašparović et al. 2018). According to Balenović et al. (2018), the error points in DTM_{PHM} could cause up to ± 4 m vertical errors. In the case that wall-to-wall mapping of forest variables is applied throughout the entire study area, it could be assumed that these vertical errors in DTM_{PHM} can cause great estimation errors. Therefore, prior to using the official Croatian digital terrain data (DTM_{PHM}) in forest inventory, it is recommended to detect and eliminate gross errors. These errors can be detected visually and eliminated manually (Balenović et al. 2018) or automatically as proposed by Gašparović et al. (2018).

4. Conclusions

As many countries worldwide, including Croatia, still do not have complete DTM coverage obtained by ALS (DTM_{ALS}), this study evaluated for the first time the applicability of the official Croatian DTM_{PHM} in the UAV-based forest inventory of lowland even-aged pedunculate oak forests. For that purpose, plot-level mean tree height (H_L) was estimated from DSM_{UAV} normalized with: (i) DTM_{ALS} , (ii) DTM_{PHM} , and (iii) DTM_{PHMc} that is corrected DTM_{PHM} for which elevation errors were eliminated. Small, almost negligible variations were obtained between H_L estimated from DSM_{UAV} normalized with three different DTMs. The results revealed that, in the absence of DTM_{ALS} , the existing official Croatian DTM_{PHM} could be readily used in remote sensing based forest inventory of lowland forest areas. It can be noted that corrected DTM_{PHMc} did not improve the accuracy of H_L estimates because gross errors did not occur in study plots. However, since the existence of gross errors in Croatian DTM_{PHM} has been confirmed by several studies, prior to using the DTM_{PHM} in forest inventory, it is recommended to detect and eliminate gross errors from digital terrain data. Additionally, comparison with the previous studies based on ALS data or digital aerial images obtained by aircraft confirmed the great potential of UAV photogrammetry in the area-based forest inventory.

Acknowledgments

This research has been fully supported by the Croatian Science Foundation under the project IP-2016-06-7686 »Retrieval of Information from Different Optical 3D Remote Sensing Sources for Use in Forest Inventory (3D-FORINVENT)«. The work of doctoral student Luka Jurjević has been supported in part by the »Young researchers' career development project – training of doctoral students« of the Croatian Science Foundation funded by the European Union from the European Social Fund. The authors wish to thank Hrvatske vode, Zagreb, Croatia for providing ALS data.

5. References

- ASPRS, 2008: LAS Specification, version 1.2. The American Society for Photogrammetry and Remote Sensing, Bethesda, Maryland, USA.
- Axelsson, P., 2000: DEM generation from laser scanner data using adaptive TIN models. *International Archives of Photogrammetry and Remote Sensing* 33(B4/1; PART 4): 111-118.
- Balenović, I., Simić Milas, A., Marjanović, H., 2017: A Comparison of Stand-Level Volume Estimates from Image-Based Canopy Height Models of Different Spatial Resolutions. *Remote Sensing* 9(3): 205.

- Balenović, I., Gašparović, M., Simic Milas, A., Berta, A., Seletković, A., 2018: Accuracy Assessment of Digital Terrain Models of Lowland Pedunculate Oak Forests Derived from Airborne Laser Scanning and Photogrammetry. *Croatian Journal of Forest Engineering* 39(1): 117–128.
- Baltsavias, E., Gruen, A., Eisenbeiss, H., Zhang, L., Waser, L.T., 2008: High-quality image matching and automated generation of 3D tree models. *International Journal of Remote Sensing* 29(5): 1243–1259.
- Bohlin, J., Wallerman, J., Fransson, J.E.S., 2012: Forest variable estimation using photogrammetric matching of digital aerial images in combination with a high-resolution DEM. *Scandinavian Journal of Forest Research* 27(7): 692–699.
- Bohlin, J., Bohlin, I., Jonzén, J., Nilsson, M., 2017: Mapping forest attributes using data from stereophotogrammetry of aerial images and field data from the national forest inventory. *Silva Fennica* 51(2): 2021.
- Coops, N.C., Hilker, T., Wulder, M., St-Onge, B., Newnham, G., Siggins, A., Trofymow, J.A., 2007: Estimating canopy structure of Douglas-fir forest stands from discrete-return LiDAR. *Trees* 21(3): 295–310.
- DeWitt, J.D., Warner, T.A., Chirico, P.G., Bergstresser, S.E., 2017: Creating high-resolution bare-earth digital elevation models (DEMs) from stereo imagery in an area of densely vegetated deciduous forest using combinations of procedures designed for lidar point cloud filtering. *GIScience & Remote Sensing* 54(4): 552–572.
- Dormann, C.F., Elith, J., Bacher, S., Buchmann, C., Carl, G., Carré, G., Marquéz, J.R., Gruber, B., Lafourcade, B., Leitão, P.J., Münkemüller, T., McClean, C., Osborne, P.E., Reineking, B., Schröder, B., Skidmore, A.K., Zurell, D., Lautenbach, S., 2013: Collinearity: a review of methods to deal with it and a simulation study evaluating their performance. *Ecography* 36(1): 27–46.
- Gašparović, M., Seletković, A., Berta, A., Balenović, I., 2017: The Evaluation of Photogrammetry-Based DSM from Low-Cost UAV by LiDAR-Based DSM. *South-east European forestry* 8(2): 117–125.
- Gašparović, M., Simic Milas, A., Seletković, A., Balenović, I., 2018: A Novel Automated Method for the Improvement of Photogrammetric DTM Accuracy in Forests. *Šumarski list* 142(11–12): 567–576.
- Gobakken, T., Bollandsås, O.M., Næsset, E., 2015: Comparing biophysical forest characteristics estimated from photogrammetric matching of aerial images and airborne laser scanning data. *Scandinavian Journal of Forest Research* 30(1): 73–86.
- Goodbody, T.R.H., Coops, N.C., Marshall, P.L., Tompalski, P., Crawford, P., 2017: Unmanned aerial systems for precision forest inventory purposes: A review and case study. *Forestry Chronicle* 93(1): 71–81.
- Guerra-Hernández, J., González-Ferreiro, E., Monleón, V.J., Faias, S.P., Tomé, M., Díaz-Varela, R.A., 2017: Use of Multi-Temporal UAV-Derived Imagery for Estimating Individual Tree Growth in *Pinus pinea* Stands. *Forests* 8(8): 300.
- Guerra-Hernández, J., Cosenza, D.N., Estraviz Rodriguez, L.C., Silva, M., Tomé, M., Díaz-Varela, R.A., González-Ferreiro, E., 2018: Comparison of ALS- and UAV(SfM)-derived high-density point clouds for individual tree detection in *Eucalyptus* plantations. *International Journal of Remote Sensing* 39(15–16): 5211–5235.
- Hill, T., Lewicki, P., 2007: STATISTICS: Methods and Applications. StatSoft, Inc.: Tulsa, OK, USA, 800 p.
- Lisein, J., Pierrot-Deseilligny, M., Bonnet, S., Lejeune, P., 2013: A photogrammetric workflow for the creation of a forest canopy height model from small unmanned aerial system imagery. *Forests* 4(4): 922–944.
- MathWorks, Inc. (2016). MATLAB: the language of technical computing: computation, visualization, programming: installation guide for UNIX version 9. Math Works Inc., Natick, MA, USA.
- McGaughey, R.J., 2018: FUSION/LDV: Software for LiDAR Data Analysis and Visualization. Version 3.80.
- Michailoff, I., 1943: Zahlenmässiges Verfahren für die Ausführung der Bestandeshöhenkurven. *Cbl. und Thar. Forstl. Jahrbuch* 6: 273–279.
- Montealegre, A.L., Lamelas, M.T., de la Riva, J., Martín, A.G., Escribano, F., 2016: Use of low point density ALS data to estimate stand-level structural variables in Mediterranean Aleppo pine forest. *Forestry* 89(4): 373–382.
- Moudrý, V., Urban, R., Štroner, M., Komárek, J., Brouček, J., Prošek, J., 2018: Comparison of a commercial and home-assembled fixed-wing UAV for terrain mapping of a post-mining site under leaf-off conditions. *International Journal of Remote Sensing*. doi: <https://doi.org/10.1080/01431161.2018.1516311>.
- Næsset, E., 1997: Determination of mean tree height of forest stands using airborne laser scanner data. *ISPRS Journal of Photogrammetry and Remote Sensing* 52(2): 49–56.
- Næsset, E., 2002: Predicting forest stand characteristics with airborne scanning laser using a practical two-stage procedure and field data. *Remote Sensing of Environment* 80(1): 88–99.
- Næsset, E., 2014: Area-Based Inventory in Norway – From Innovation to an Operational Reality. In: *Forestry Applications of Airborne Laser Scanning. Managing Forest Ecosystems (Maltamo M., Næsset E., Vauhkonen J., eds.)*, Springer, Dordrecht, 215–240 p.
- Nurminen, K., Karjalainen, M., Yu, X., Hyyppä, J., Honkavaara, E., 2013: Performance of dense digital surface models based on image matching in the estimation of plot-level forest variables. *ISPRS Journal of Photogrammetry and Remote Sensing* 83: 104–115.
- Ørka, H.O., Bollandsås, O.M., Hansen, E.H., Næsset, E., Gobakken, T., 2018: Effects of terrain slope and aspect on the error of ALS-based predictions of forest attributes. *Forestry* 91(2): 225–237.
- Ota, T., Ogawa, M., Mizoue, N., Fukumoto, K., Yoshida, S., 2017: Forest Structure Estimation from a UAV-Based Photo-

- grammetric Point Cloud in Managed Temperate Coniferous Forests. *Forests* 2017 8(9): 343.
- Pitt, D.G., Woods, M., Penner, M., 2014: A Comparison of Point Clouds Derived from Stereo Imagery and Airborne Laser Scanning for the Area-Based Estimation of Forest Inventory Attributes in Boreal Ontario. *Canadian Journal of Remote Sensing* 40(3): 214–232.
- Puliti, S., Ørka, H.O., Gobakken, T., Næsset, E., 2015: Inventory of Small Forest Areas Using an Unmanned Aerial System. *Remote Sensing* 7(8): 9632–9654.
- Puliti, S., Gobakken, T., Ørka, H.O., Næsset, E., 2016: Assessing 3D point clouds from aerial photographs for species-specific forest inventories. *Scandinavian Journal of Forest Research* 32(1): 68–79.
- Puliti, S., Ene, L.T., Gobakken, T., Næsset, E., 2017: Use of partial-coverage UAV data in sampling for large scale forest inventories. *Remote Sensing of Environment* 194: 115–126.
- Rahlf, J., Breidenbach, J., Solberg, S., Astrup, R., 2015: Forest Parameter Prediction Using an Image-Based Point Cloud: A Comparison of Semi-ITC with ABA. *Forests* 6(11): 4059–4071.
- Rahlf, J., Breidenbach, J., Solberg, S., Næsset, E., Astrup, R., 2017: Digital aerial photogrammetry can efficiently support large-area forest inventories in Norway. *Forestry* 90(5): 710–718.
- Smreček, R., Michnová, Z., Sačkov, I., Danihelová, Z., Levická, M., Tuček, J., 2018: Determining basic forest stand characteristics using airborne laser scanning in mixed forest stands of Central Europe. *iForest* 11: 181–188.
- Stepper, S., Straub, C., Pretzsch, H., 2015: Using semi-global matching point clouds to estimate growing stock at the plot and stand levels: Application for a broadleaf-dominated forest in central Europe. *Canadian Journal of Forest Research* 45(1): 111–123.
- Straub, C., Stepper, C., Seitz, R., Waser, L.T., 2013: Potential of UltraCamX stereo images for estimating timber volume and basal area at the plot level in mixed European forests. *Canadian Journal of Forest Research* 43(8): 731–741.
- Terrasolid Ltd., 2012: Terrascan. <http://www.terrasolid.fi/en/products/terrascan>.
- Tuominen, S., Balazs, A., Saari, H., Pölönen, I., Sarkeala, J., Viitala, R., 2015: Unmanned aerial system imagery and photogrammetric canopy height data in area-based estimation of forest variables. *Silva Fennica* 49(5): 1348.
- Tuominen, S., Balazs, A., Honkavaara, E., Pölönen, I., Saari, H., Hakala, T., Viljanen, N., 2017: Hyperspectral UAV-imagery and photogrammetric canopy height model in estimating forest stand variables. *Silva Fennica* 51(5): 7721.
- Vastaranta, M., Wulder, M.A., White, J.C., Pekkarinen, A., Tuominen, S., Ginzler, C., Kankare, V., Holopainen, M., Hyypä, J., Hyypä, H., 2013: Airborne laser scanning and digital stereo imagery measures of forest structure: Comparative results and implications to forest mapping and inventory update. *Canadian Journal of Remote Sensing* 39(5): 382–395.
- Ullah, S., Dees, M., Datta, P., Adler, P., Koch, B., 2017: Comparing Airborne Laser Scanning, and Image-Based Point Clouds by Semi-Global Matching and Enhanced Automatic Terrain Extraction to Estimate Forest Timber Volume. *Forests* 8(6): 215.
- Wallace, L., Lucieer, A., Malenovský, Z., Turner, D., Vopěnka, P., 2016: Assessment of Forest Structure Using Two UAV Techniques: A Comparison of Airborne Laser Scanning and Structure from Motion (SfM) Point Clouds. *Forests* 7(3): 62.
- White, J.C., Wulder, M.A., Vastaranta, M., Coops, N.C., Pitt, D., Woods, M., 2013: The Utility of Image-Based Point Clouds for Forest Inventory: A Comparison with Airborne Laser Scanning. *Forests* 4(3) 518–536.
- White, J.C., Coops, N.C., Wulder, M.A., Vastaranta, M., Hilker, T., Tompalski P., 2016: Remote Sensing Technologies for Enhancing Forest Inventories: A Review. *Canadian Journal of Remote Sensing* 42(5): 619–641.
- Yu, X., Hyypä, J., Holopainen, M., Vastaranta, M., 2010: Comparison of Area-Based and Individual Tree-Based Methods for Predicting Plot-Level Forest Attributes. *Remote Sensing* 2(6): 1481–1495.
- Zimmermann, S., Hoffmann, K., 2017: Accuracy Assessment of Normalized Digital Surface Models from Aerial Images Regarding Tree Height Determination in Saxony, Germany. *PFG – Journal of Photogrammetry, Remote Sensing and Geoinformation Science* 85(4): 257–263.

Authors' addresses:

Ivan Balenović, PhD *

e-mail: ivanb@sumins.hr

Luka Jurjević, mag. ing. geod. et geoinf.

e-mail: lukaj@sumins.hr

Danijela Ivanković, dipl. ing. šum.

e-mail: danijela@sumins.hr

Division for Forest Management and

Forestry Economics

Croatian Forest Research Institute

Trnjanska cesta 35

Zagreb

CROATIA

Asst. prof. Anita Simic Milas, PhD

e-mail: asimic@bgsu.edu

School of Earth, Environment and Society

Bowling Green State University

190 Overman Hall

Bowling Green, OH

USA

Asst. prof. Mateo Gašparović, PhD

e-mail: mgasparovic@geof.hr

Chair of Photogrammetry and Remote Sensing

Faculty of Geodesy, University of Zagreb

Kačićeva 26

Zagreb

CROATIA

Assoc. prof. Ante Seletković, PhD

e-mail: aseletkovic@sumfak.hr

Department of Forest Inventory and Management

Faculty of Forestry University of Zagreb

Svetošimunska 25

Zagreb

CROATIA

* Corresponding author

Received: September 28, 2018

Accepted: December 04, 2018